Electronic Supplementary Information for

Photochromism in the periodic nanospace of zeolite LTA by the transfer of photoexcited electrons of adsorbed Na atoms

Tetsuya Kodaira[1] and Takuji Ikeda[2]

[1]National Institute of Advanced Industrial Science and Technology (AIST), 1-1-1 Higashi, Tsukuba, Ibaraki 305-8565, Japan

[2]National Institute of Advanced Industrial Science and Technology (AIST), 4-2-1 Nigatake, Miyagino, Sendai, 983-8551, Japan

Corresponding author: Tetsuya Kodaira (kodaira-t@aist.go.jp)

Table of Contents

Abbreviations used in the main article and the Supporting Information.

Na-LTA:	Na-form alumino-silicate type zeolite **LTA** with Si/Al = 1.
Na-LTA(s):	Na-LTA with severe dehydration.
Na-LTA(m):	Na-LTA with mild dehydration.
Na/Na-LTA(s or m):	Na-LTA(s or m) with adsorbed Na.
pUC:	Pseudo unit cell which includes one α- and one β-cages. ($Na_{12}Al_{12}Si_{12}O_{48}$, lattice constant $a_{pUC} \approx 1.23$ nm.)
Electron:	The doped electron in the nanospace of dehydrated Na-LTA by adsorbing Na atoms.
HFS:	Hyperfine structure.
PXRD:	Powder X-ray diffraction.
SEM:	Scanning electron microscope.
FT-IR:	Fourier-transform infrared (spectroscopy).
TG-DTA:	Thermogravimetry and differential thermal analysis.
DR:	Diffuse reflection (reflectance).
ESR:	Electron spin resonance.

S1. Zeolite LTA.

The framework structure of **LTA** shown in **Fig. 1** is described in this section. Zeolite **LTA** has two kinds of cages, *i.e.*, α- and β-cages, which are often called supercages and sodalite cages, respectively. Both consist of a simple cubic array. α-cages (inner diameter of 1.10–1.15 nm) are directly connected by sharing 8-rings (8R), but β-cages (inner diameter of 0.65–0.70 nm) are mutually isolated by double 4-rings (D4R). α- and β-cages share 6-rings (6R).

The locations and their occupancies of charge-compensating alkali metal cations for a negatively charged alumino-silicate framework to neutralize the crystal depend on their kinds and the framework Si/Al atomic ratios. The most popular and commercially available zeolite **LTA** has an Si/Al atomic ratio of unity. Locations and their occupancies by the Na^+ ions at this **LTA** are explained in the main article. Zeolite **LTA**s with Si/Al > 1 are also known.[S1–S4] On these **LTA**s, 6R sites are preferable for Na^+ ions,[S5] while 8R sites are preferable for K^+ ions.[S6]

S2. Characterizations of Na-LTA before Na adsorption.

S2.1 As-synthesized Na-LTA.

The PXRD pattern (**Fig. S1**) indicates that the Na-LTA was a single phase with no byproducts, e.g., faujasite (**FAU**). The lattice constant was determined as a = 2.46091(2) nm (space group: $Fm\bar{3}c$) using the whole pattern profile-fitting method. The crystals had cubic morphology with ridges cut off with an average size of *ca*. 3 μm (**Fig. S2**).

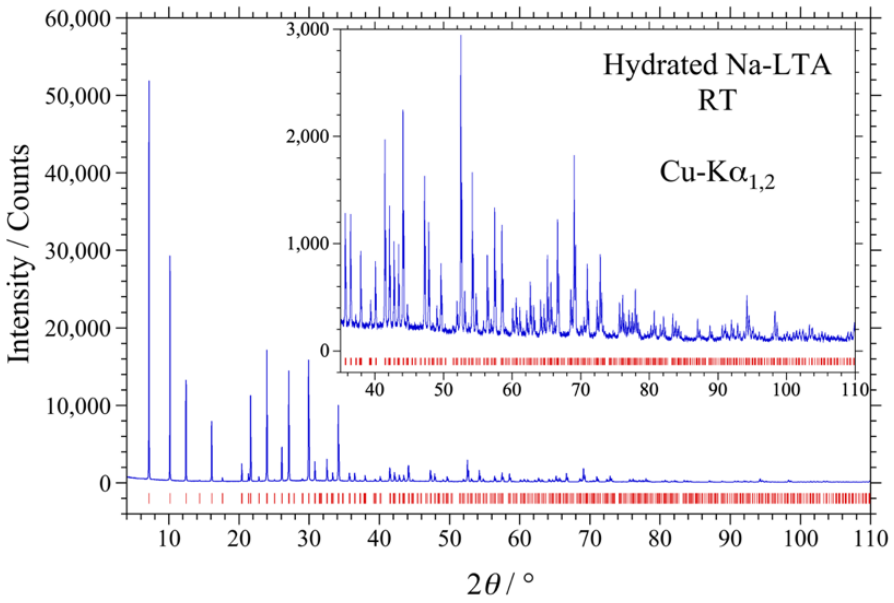

Fig. S1 The PXRD pattern of as-synthesized (hydrated) Na-LTA. Bars under the pattern indicate the positions of allowed reflections for the space group $Fm\bar{3}c$ with a lattice constant of 2.46091 nm. The inset is the magnified pattern of 2θ = 35–110° for the vertical axis direction.

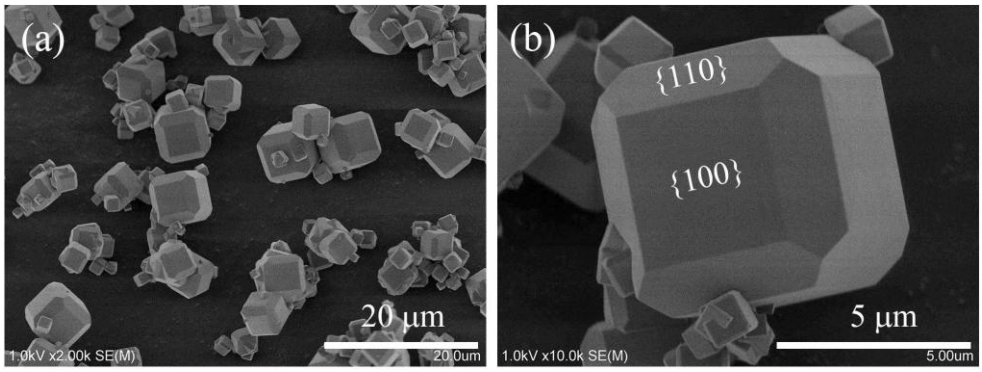

Fig. S2 SEM images of as-synthesized Na-LTA. Magnifications are (a) 2k and (b) 10k. A magnified image of the largest crystal is shown in (b).

Because no organic structural directing agent was used for the synthesis, the TG-DTA curves of Na-LTA crystals merely exhibited weight loss due to dehydration, giving endothermic peaks (**Fig. S3**). Most water molecules could be removed by elevating the temperature to 700 K. However, as alkali metals are extremely reactive with residual water, the dehydrating conditions affected the incorporated Na species in the nanospace of Na-LTA, as described in the main article. From the TG curve, the number of initially adsorbed water molecules was estimated to be 27.2 per pUC, *i.e.*, $Na_{12}Al_{12}Si_{12}O_{48}\cdot 27.2H_2O$.

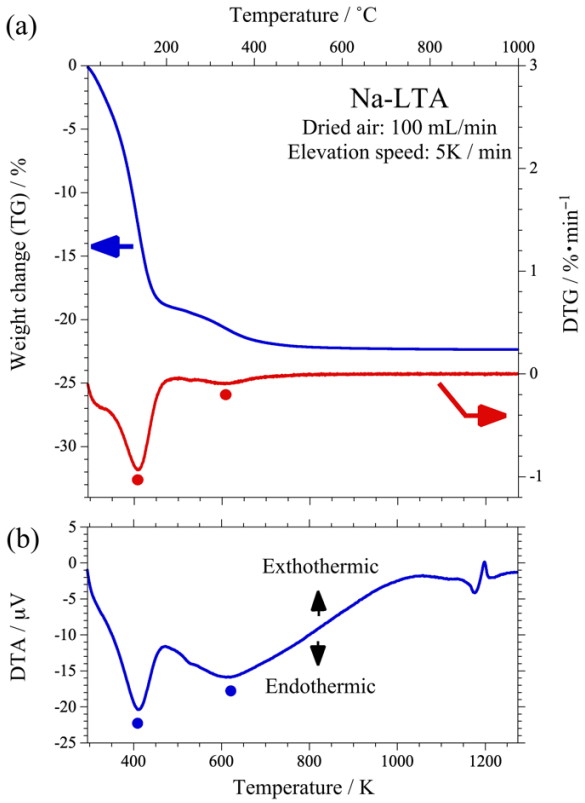

Fig. S3 TG-DTA results of hydrated Na-LTA. (a) TG and differential TG (DTG) curves and (b) a DTA curve. The temperatures at the closed circles in the DTG curve coincide with the endothermic temperatures in the DTA curve.

S2.2 FT-IR spectra of Na-LTA samples.

Considering the chemical formula of hydrated and dehydrated Na-LTA ($Na_{12}Al_{12}O_{48}\cdot xH_2O$@pUC), the stretching modes of hydroxyl groups (–OH) are the sole observable vibrational transitions in the measured wavenumber region 2300–4500 cm^{-1}. Namely, water molecules, Brönsted acid points and silanol groups are the candidates for the transition origins.

Figure 2 in the main article shows the FT-IR spectra of Na-LTA samples. Hydrated Na-LTA shows a broad single absorption profile whose peak position is ca. 3500 cm^{-1}. Abundant water molecules adsorbed in the cages of Na-LTA are the origin of this absorption. At Na-LTA(m), the peak intensity of this photoabsorption was weakened to less than one-hundredth by dehydration, indicating that the major portion of the water molecules was removed. The sharp peak at 3723 cm^{-1} was made clear by the dehydration. This peak might have arisen due to the smaller mutual interaction of hydrogen bonds among the residual water molecules. In support of this interpretation, a very small amount of residual water molecules was detected in β-cages by analysis of the PXRD pattern of dehydrated Na-LTA using Rietveld refinement combined with the maximum entropy method.[S7] The silanol groups, whose stretching mode appears at 3742 cm^{-1}, are known to be stable up to 900 K,[S8] but this peak was weakened at Na-LTA(s), whose dehydrating temperature was 773 K.

The wavenumbers of the absorption peaks in the FT-IR spectra of dehydrated Na-LTAs are discussed. Isolated water molecules ($H_2{}^{16}O$) in a vapor phase have an asymmetric stretching mode at 3756 cm^{-1} and a symmetric mode at 3657 cm^{-1}.[S9] The observed absorption peaks in the FT-IR spectra have smaller wavenumbers than the asymmetric mode of the molecules in the vapor. This indicates that the residual water molecules apparently have interactions with Na-LTA which cannot be ignored. In particular, hydrogen and oxygen atoms of the residual water molecules interact attractively with oxygen atoms of the framework and the Na^+ ions, respectively. Na-LTA(s) includes far fewer water molecules than Na-LTA(m) as can be seen in the figure, and the spectral shape did not change proportionally with the further dehydration. This variation of the spectral shape suggests that several adsorption states are for the residual water molecules. In the present, it is difficult to determine the detailed vibrational modes of them.

S3. Measurement details.

S3.1 DR spectra.

- **DR spectra under light irradiation**

DR spectra before and under the excitation light irradiation were obtained and compared using the optical configuration illustrated in **Fig. S4**. The monochromatized probe light of the tungsten halogen lamp was scanned for 1160–300 nm to obtain DR spectra. The wavelength of the excitation light was fixed to *ca*. 390 nm and was continuously irradiated to the sample. Although DR light from the sample includes both probe and excitation light source components, only the signal from the probe light could be obtained, because the probe light was modulated with the optical chopper operated at 75 Hz, and the lock-in amplifier extracted and outputted the electric component modulated at that frequency only. A photomultiplier tube and a Si photodiode were used as detectors for 300–800 nm and 600–1160 nm, respectively. Finally, the two spectra were combined into one spectrum. In some cases, a quartz glass cryostat was used to cool the sample down to 77 K by soaking the sample in liquid nitrogen.

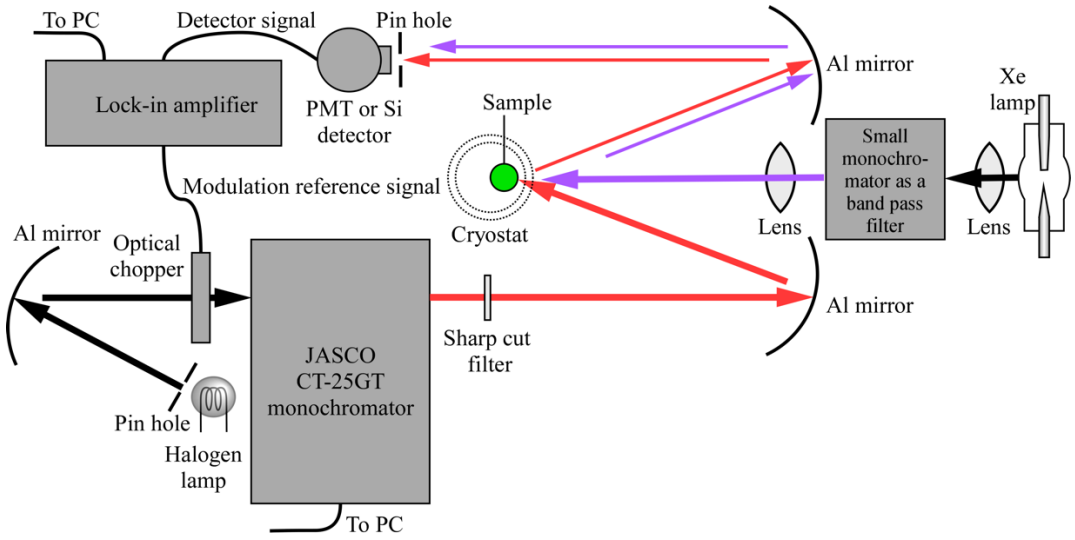

Fig. S4 The system to measure a DR spectrum under additional light irradiation to a sample.

- **Dependence of DR spectra on the light irradiation duration**

The system shown in **Fig. S4** enables us to measure the spectrum of the equilibrium photoinduced state (photochromism) under light irradiation. As the system requires a scan of at least 10 min to obtain one spectrum, it was impossible to detect the dynamic changes in the spectra within the a few minutes after the start of the light irradiation. Thus, a new optical system was set up as follows.

In the system depicted in **Fig. S5**a, white probe light was irradiated to the sample directly. To suppress the photochromism and to keep the probe light from heating up the sample, light of unneeded wavelengths was eliminated by inserting a sharp cut or a band pass filter before the irradiation to the sample. The DR light from the probe was collected and introduced to the polychromator equipped with a photodiode array of 1020 channels. DR light from the monochromatized Xe lamp, which was irradiated to the sample to induce photochromism, was also at risk of being introduced into the polychromator. In order to prevent this, two optical choppers were set in front of the polychromator (Chopper 1) and in the irradiation Xe lamp beam line (Chopper 2). They were operated at 75 Hz in antiphase (**Fig. S5**b), *i.e.*, when one was open, the other was closed. By using this technique, the Xe lamp light was never directed into the polychromator. The minimum time-resolution was one second, which was controlled by varying the light exposure time of the diode array. Spectra measured at 77 K were obtained by soaking the

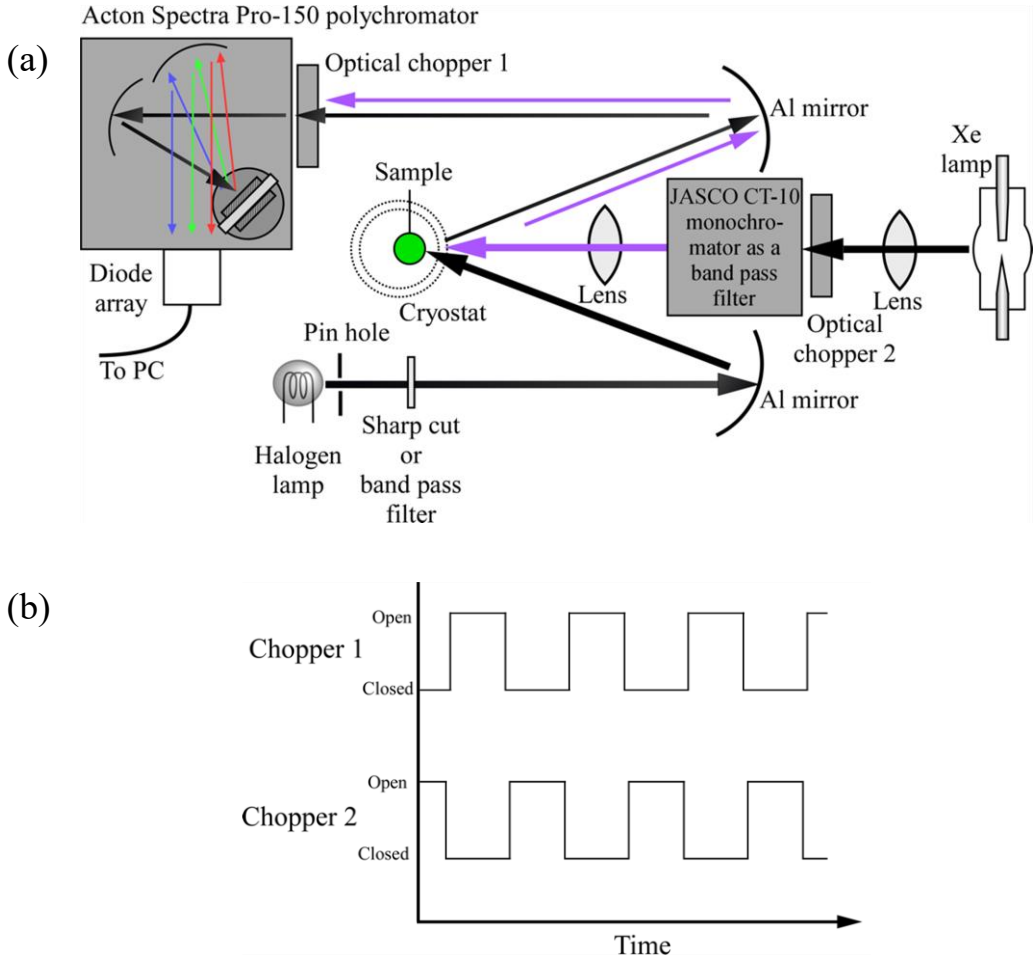

Fig. S5 (a) The system to measure time-dependent DR spectra on the irradiating time of the Xe lamp light. (b) Relative phase of the two choppers 1 and 2.

sample tube in the glass cryostat filled with liquid nitrogen. Because the polychromator we used cannot measure the full range from 300 to 1100 nm (1.1–4.0 eV) at one time, we split the range into two smaller components, *e.g.* 300–500 and 500–1100 nm, and carried the experiment out twice.

- **Ordinary DR spectra**

An Agilent Cary5000 UV-vis.-IR spectrometer was used to measure the DR spectra when the additional excitation light to induce the photochromism was unnecessary during the measurements. The measurement of the DR spectra was realized by setting up the DR optical configuration for the probe light in a similar manner to that depicted in **Figs. S4** and **S5** using two concave Al mirrors, *i.e.,* leading monochromatized light out of the apparatus and giving back the DR light from the sample to the apparatus again to be detected.

S3.2 ESR

An X-band (≈ 9.5 GHz microwave) ESR apparatus, Bruker ESP300E, was used to obtain spectra in the first derivative mode. The apparatus was equipped with a Gauss meter to detect magnetic field values and a microwave frequency counter. Blue light from light-emitting diodes (LEDs) with a peak wavelength of 400 ± 5 nm (3.1 eV) or monochromatized Xe lamp light using a band pass filter of 230 nm (5.5 eV) were introduced into the ESR cavity through its optical windows. For the low temperature measurement, an ESR900 cryostat (Oxford Instruments) was used. Detailed conditions of the measurements are listed in **Table S1**.

S3.3 Fundamental analysis

- **PXRD**

The PXRD pattern of our synthesized Na-LTA was collected under ambient conditions by using a Rigaku SmartLab X-ray diffractometer in the Bragg-Brentano geometry with Cu-Kα radiation. The apparatus was equipped with a CBO-α multilayer mirror suppressing Cu-Kβ radiation, Soller slits with a divergence angle of 1.0˚, and a D/teX Ultra 250, which is a high-speed 1D silicon strip X-ray detector.

The PXRD pattern of the Na/Na-LTA(s) sample could not be measured under an atmospheric condition. Therefore, the powder sample in the glass tube had to be charged and sealed in a borosilicate glass capillary tube of 0.5ϕ without exposing it to the air by using an N_2 gas glove box manufactured by Miwa (O_2 and $H_2O \leq 1$ ppm). The PXRD pattern of Na/Na-LTA(s) was measured with a modified Debye–Scherrer geometry at RT using a PANalytical Empyrean diffractometer equipped with a primary monochromator

and a focusing mirror providing Cu-Kα_1 radiation, Soller slits of a 2.3˚ divergent angle and the GaliPIX^{3D} two-dimensional detector.

- **SEM**

SEM images were obtained with a Hitachi S4800 equipped with a field emission electron gun. The acceleration voltage of the incident beam was 1.0 kV, and secondary electrons from the sample were detected.

- **FT-IR**

FT-IR DR spectra of the samples sealed in quartz glass tubes were obtained using a Nicolet Magna-IR 750. The apparatus was equipped with a halogen lamp, a CaF_2 beam splitter, and a PbSe detector. The spectral resolution was set to 8 cm^{-1}. KCl powder in a quartz glass tube was used as a standard sample. It was impossible to obtain a spectrum below 2200 cm^{-1} because of the strong photoabsorption from the quartz glass tube.

- **TG-DTA**

TG-DTA curves were obtained using a Rigaku Thermo plus EVO2 TG-DTA8120. About 10 mg of hydrated Na-LTA was set in a Pt holder. The measurement was conducted using a temperature elevation speed of 5 K/min and a dried air gas supply of 100 cm^3/min. α-Al_2O_3 in a Pt holder was used as a reference sample of DTA.

- **Stereomicroscope observation**

A stereomicroscope Olympus SZX10 equipped with a CMOS camera was used to obtain time-lapse images of the samples. Representative images were extracted from the time-lapse series to demonstrate the color variation. White LED light was used for lighting. Photochromism was induced by the white LED light itself for Na/Na-LTA(s) and by the white LED light plus a D_2 lamp light for Na/Na-LTA(m).

S4. Na-adsorbed Na-LTA(s) (Na/Na-LTA(s)).

S4.1 Crystallinity of Na/Na-LTA(s) and the adsorbed amounts of Na atoms.

Figure S6 shows the optical absorption spectrum of Na/Na-LTA(s) with ca. 1.0 Na atoms adsorbed per pUC. Non-ground Na-LTA was used. The sample was completely black, and the appearance of S_1 and S_2 bands corresponds with the findings of the previous work.[S10] The spectral region at photon energies higher than 1.8 eV is inaccurate because of the strong absorption. Ground Na-LTA was used to obtain the spectra in **Fig. 4**. The appearance of common S_1 and S_2 bands in the spectra of sample (e) in **Fig. 4** and **Fig. S6** indicates that the grinding of Na-LTA did not damage its crystallinity but merely reduced the average size of the crystal size, thereby suppressing the photoabsorption intensity.

From the similarity of these two spectra, the sample (e) in **Fig. 4** can be treated as including a similar amount of adsorbed Na atoms. By assuming that the spectral area at 1.1–3.8 eV in **Fig. 4** is in proportion to the adsorbed Na amount, we could derive the adsorbed amounts of Na atoms as described in the main article. The above-described confirmation that the crystallinity was maintained by grinding and the estimations of Na-adsorbing amounts are based on the assumptions that the **LTA** structure was preserved after the dehydration and the Na adsorption. For this reason, the crystal structure of the sample used to obtain the spectrum in **Fig. S6** was evaluated. The Na/Na-LTA(s) powder sample in a sealed glass tube was charged into a 0.5ϕ borosilicate glass capillary tube and sealed again without exposing it to air using an N_2 gas globe box (O_2 and $H_2O \approx 1$ ppm). The PXRD pattern was measured in a transmission geometry with the Cu-Kα_1 line as

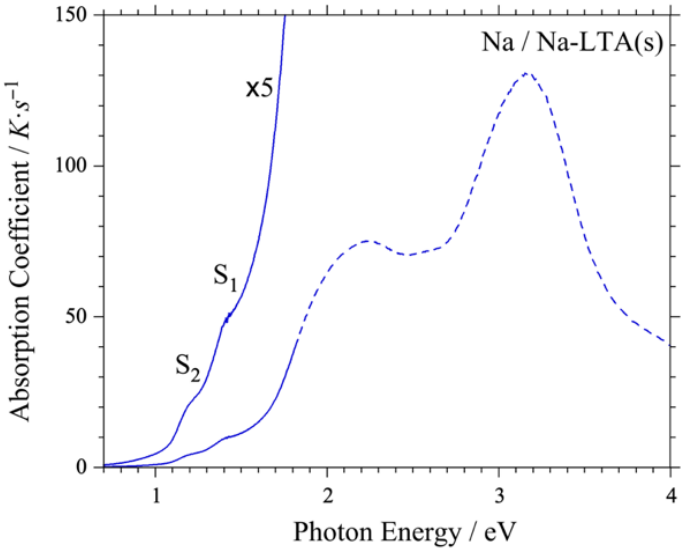

Fig. S6 Optical absorption spectrum of the Na/Na-LTA(s) with *ca.* 1.0 Na atoms adsorbed per pUC measured at RT. This sample was used for the measurement of the PXRD pattern in **Fig. S7**.

explained in Section S3.3 of this ESI. No peak splitting of initial reflections of hydrated Na-LTA was observed, and no new reflections were observed (**Fig. S7**). All the reflections could be indexed by the initial space group of $Fm\bar{3}c$ with the lattice constant of a = 2.45791(2) nm. This result guarantees that the **LTA** framework structure was maintained in all samples appearing in this article. The lattice constant of this sample was slightly shortened compared to that of hydrated Na-LTA, a = 2.46091(2) nm (see Section S2.1 in this ESI).

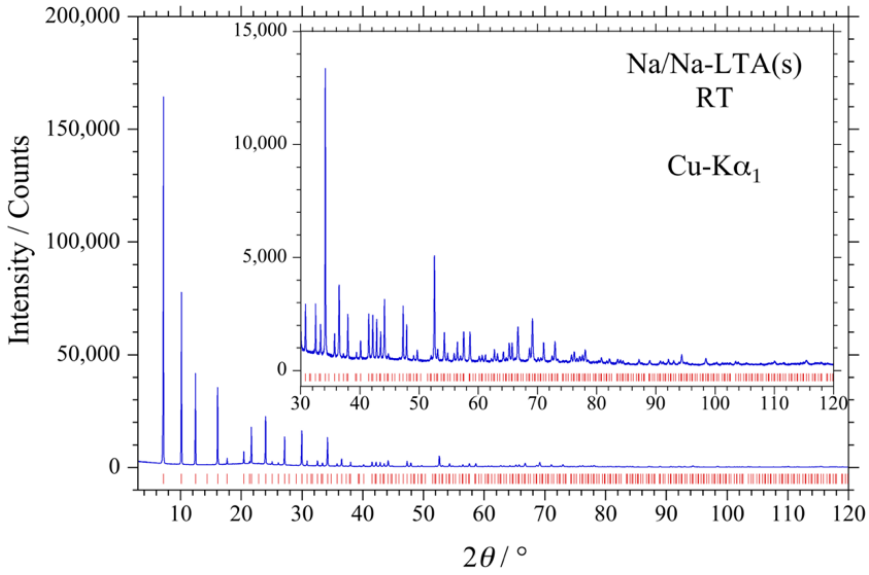

Fig. S7 PXRD pattern of Na/Na-LTA(s) with *ca*. 1.0 atoms per pUC. Bars under the pattern indicate the positions of allowed reflections for the space group $Fm\bar{3}c$ with a lattice constant of 2.45791 nm. The inset is the pattern of 2θ = 30–120° magnifying the vertical axis direction.

S4.2 Dependence of the spectral shape on temperature.

Although no photochromism could be observed by light irradiation whose photon energy was resonated to D_1 and D_2 bands at 77 K, the spectral width of the D_1 and D_2 bands was found to be narrowed, as shown in **Fig. S8**. This is direct evidence of the presence of the electron–phonon interaction, *i.e.*, the electron of the Na clusters in β-cages coupled with the vibration/displacement of Na^+ ions of the Na clusters in the present case. This kind of spectral width-dependence on temperature can be observed at the optical spectra of F centers in alkali-halides.[S11]

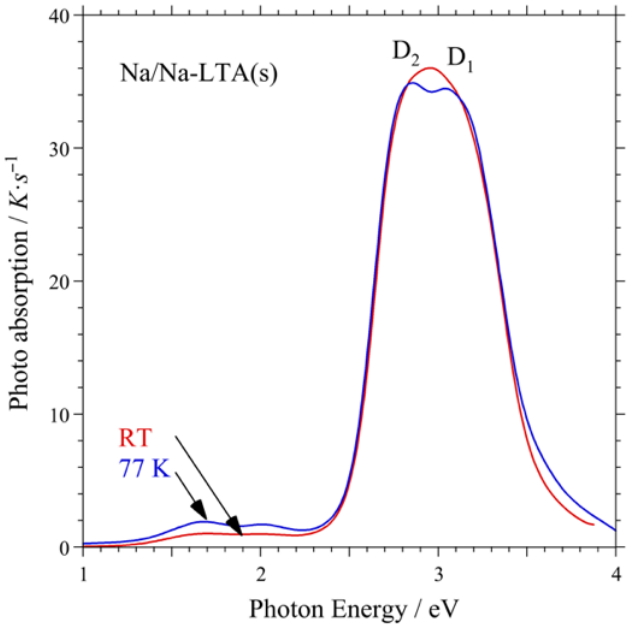

Fig. S8 Absorption spectra of Na/Na-LTA(s) measured at RT (red) and 77 K (blue). The adsorbed amount of Na atoms of this sample corresponds to the intermediate of the samples (b) and (c) in **Fig. 4** in the main article.

S4.3 Estimation of the amount of Na atoms adsorbed in Na-LTA(s).

The photoabsorption spectrum of the Na/Na-LTA(s), which was used for the ESR measurement shown in **Fig. 5** in the main article, is plotted in **Fig. S9**. We can see that very weak absorption existed at 1.5–2.3 eV before the application of light irradiation to the sample. This finding indicates that a very small amount of photoinduced species was already present.

The amount of adsorbed Na atom in the sample in **Fig. S9** was estimated by applying the previous method.[S12] Namely, we adopted Smakula's equation for photoabsorption of impurity centers in a transparent matrix: [S13]

$$\int K_{\mathrm{i}}\, dE = \frac{2\pi^2 e^2 \hbar}{mc} \cdot \frac{(\varepsilon+2)^2}{9} \cdot \frac{N f_{\mathrm{i}}}{\sqrt{\epsilon}} \quad . \tag{S-1}$$

In this equation, K_{i} and f_{i} are the absorption coefficient and the oscillator strength (transition probability) of a focused photoabsorption band, respectively, and N is a number density of the centers. ε is the dielectric constant of the matrix. e, m, and c are the elementary electric charge, the mass of the electron, and the velocity of light, respectively. In the following method, we would like to determine the N which corresponds to the density of 3s electrons of adsorbed Na.

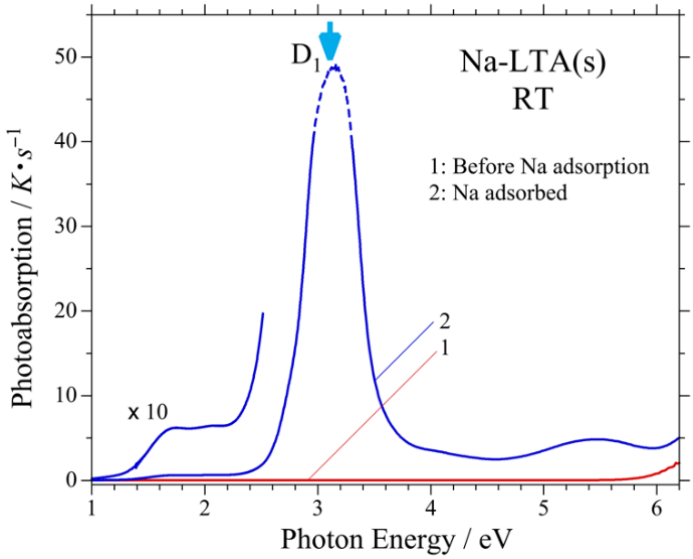

Fig. S9 Photoabsorption spectra of Na/Na-LTA(s) (blue spectrum). The downward arrow indicates the photon energy of the LED, when the photoinduced ESR spectrum was measured. The red spectrum indicates the spectra of Na-LTA(s).

The absorption coefficient K can be derived from the relationship between K and $A_{K\text{-}M}$ described in the main article, *i.e.*,

$$K(E) = A_{K-M}(E) \cdot s. \quad \text{(S-2)}$$

Because band D_1 is dominant in this spectrum (**Fig. S9**), its oscillator strength f can be approximated as unity. Other parameters of Na-LTA were settled as dielectric constant $\varepsilon = 2$ and average crystal size $s^{-1} = 3$ μm, respectively. The photoabsorption area of 2.5–3.8 eV was derived as

$$\int_{2.5}^{3.8} A_{K-M}(E) \cdot s dE = 1 \cdot 10^4 \text{ eV} \cdot \text{cm}^{-1}. \quad \text{(S-3)}$$

From Eqs. (S-1) and (S-3), the number density of electrons, N_e, contributing to the band D_1 transition can be derived as $N_e = 4 \times 10^{19}$ cm^{-3}. As the number density of β-cages is $N_\beta = 5 \times 10^{20}$ cm^{-3}, the number of electrons participating in the cluster formation per β-cage can be derived as

$$N_e/N_\beta \ (= \text{adsorbed Na atoms per pUC}) \approx 0.1. \quad \text{(S-4)}$$

This estimated value is consistent with the estimated adsorption amounts for the samples in **Fig. 4** in the main article, because no D_2 band appeared in **Fig. S9**, but a D_2 band was observed in the spectrum of the sample (a) in **Fig. 4**, whose adsorption density of Na atoms was *ca*. 0.2 per pUC.

S4.4 Estimating the number density of unpaired electrons in the sample.

Table S1 Conditions to obtain the ESR spectra before and during the light irradiation. (**Fig. 5** (a) in the main article)

Sample amount /mol of b-cage	Modulation amplitude /G	Modulation freiquency /kHz	Receiver gain	Microwave power /mW	Microwave frequency /GHz	Number of scans
$2.58\text{x}10^{-5}$	2.0	100	$5.0\text{x}10^{4}$	4.0	9.5965±0.0005	49

The number density of unpaired electrons in Na/Na-LTA(s), whose optical spectrum is shown in **Fig. S9**, was evaluated using its ESR spectrum before light irradiation (**Fig. 5**a). For this purpose, the ESR spectrum of copper(II) sulfate pentahydrate ($CuSO_4 \cdot 5H_2O$) crystal, which gives a paramagnetic property of S = ½, was recorded as shown in **Fig. S10**. The numbers of paramagnetic species, N_{para}, *i.e.*, unpaired electrons, in Na/Na-LTA(s) per β-cage (pUC) could be derived as

$$N_{\text{para}}/N_{\beta} = 4 \times 10^{-4} \qquad \text{(S-5)}$$

by comparing the ESR spectral area, *i.e*. the microwave absorption, of Na/Na-LTA(s) and $CuSO_4 \cdot 5H_2O$ crystal with consideration for the differences in receiver gain, microwave power and number of scans on the measurements and the sample amounts. The obtained values of (S-4) and (S-5) differed more than 100-fold. Thus, we can conclude that the majority of the 3s electrons of the adsorbed Na atoms form a spin singlet state in β-cages, indicating diamagnetism.

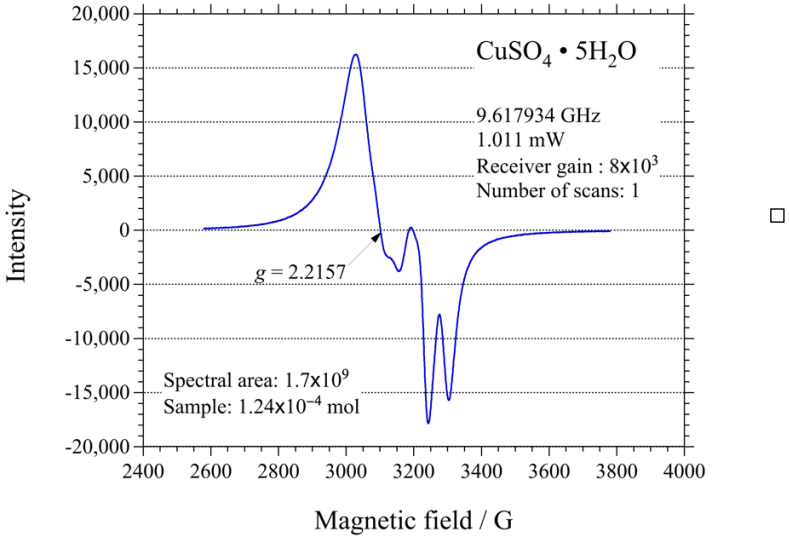

Fig. S10 The ESR spectrum of $CuSO_4 \cdot 5H_2O$ at RT. Measurement conditions that differ from those in **Table S1** are described in the figure.

S4.5 Simulation of the photoinduced ESR spectrum.

In the case of an unpaired electron (S = 1/2) interacting with n_1 equivalent nuclei with a spin of I_1 through the Fermi contact interaction, equally spaced $2n_1I_1 + 1$ lines of HFS can be observed. If additional n_2 nuclei with a different nucleus spin (I_2) and/or a different magnitude of the Fermi contact interaction exist, then the total numbers of HFS can be expressed as $(2n_1I_1 + 1) \times (2n_2I_2 + 1)$.[S14] Thus, as shown in **Scheme S1**, a total of 40 lines can be observed in the present model.

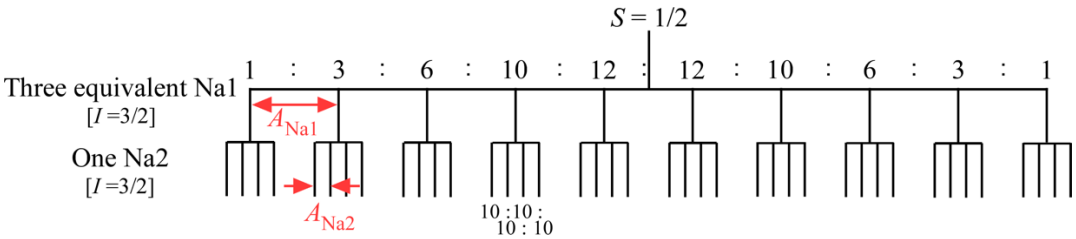

Scheme S1 Feature of the HFSs with three equivalent nuclei and one minor nucleus, both having I = 3/2 nucleus spin of Na, whose HFS coupling constants are A_{Na1} and A_{Na2}, respectively. 40 (=10 × 4) lines of HFS are observable in principle. The relative intensities of the HFS lines are also shown in the drawing.

Table S2 Parameters used for the simulation of the photoinduced ESR spectrum in **Fig. S11**. The simulated spectrum was calculated using the simulation software package SimFonia (ver. 1.25; Bruker) in solution mode.

Label	Numbers of equivalent nuclei	Nuclear spin (abundance)	HFS coupling constant, A / G
Na1	3	3/2 (100 %)	36.8
Na2	1	3/2 (100 %)	5.8
g-factor	Microwave frequency / GHz	Lorenzian/ Gausian	Line width / G
2.00232	9.5970	0	6.7

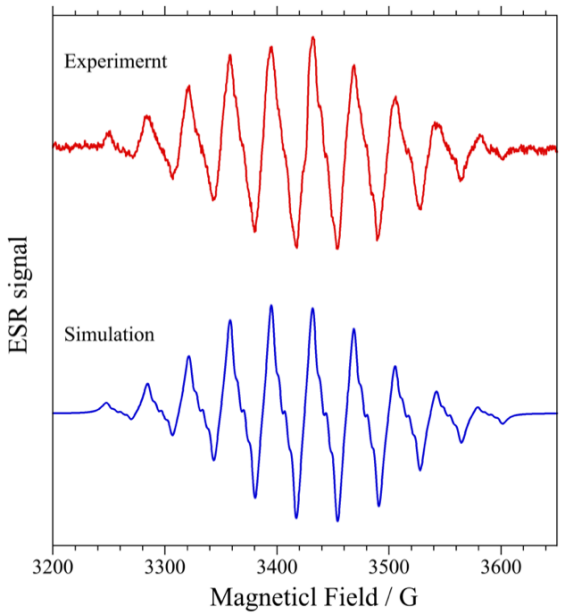

Fig. S11 Experimental and simulated spectra of the photoinduced ESR components observed at RT.

S5. Na-adsorbed Na-LTA(m) (Na/Na-LTA(m)).

S5.1 Deconvolution of photoinduced absorption bands.

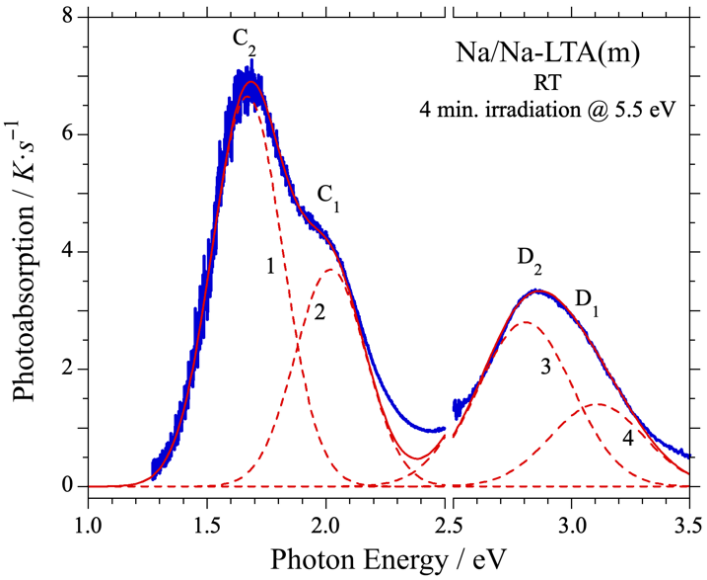

Fig. S12 Profile fitting for the photoabsorption spectrum of Na/Na-LTA(m) at UV light (5.5 eV) irradiation for 4 min at RT (extracted from **Fig. 6**a in the main article). The blue spectrum is the raw data. The dotted red profiles are the components, and the solid red profile is the total profile. Fitting parameters are listed in **Table S3**.

Table S3 Fitting parameters for the spectrum shown in **Fig. S12**. The Gauss function profile was adopted on the fitting.

	Peak position / eV	FWHM / eV	Relative absorption area
1 (C_2)	1.67	0.42	1.80
2 (C_1)	2.02	0.42	1
3 (D_2)	2.807	0.56	1.01
4 (D_1)	3.11	0.56	0.50

S5.2 Color of Na/Na-LTA(m) after terminating the UV light irradiation.

As depicted in **Fig. 10**a, the cessation of the UV light irradiation changed the color of Na/Na-LTA(m) from dark-green to lighter green, then brilliant-yellow green, then yellow, and finally light yellow. Since the sample readily changed to a greenish color in only a few seconds under normal room light, the sample had to be kept in the dark, and these images were obtained within a second of the LED light illumination to prevent photochromism by surplus irradiation.

S5.3 ESR spectrum of Na/Na-LTA(m) at 80 K under UV light irradiation.

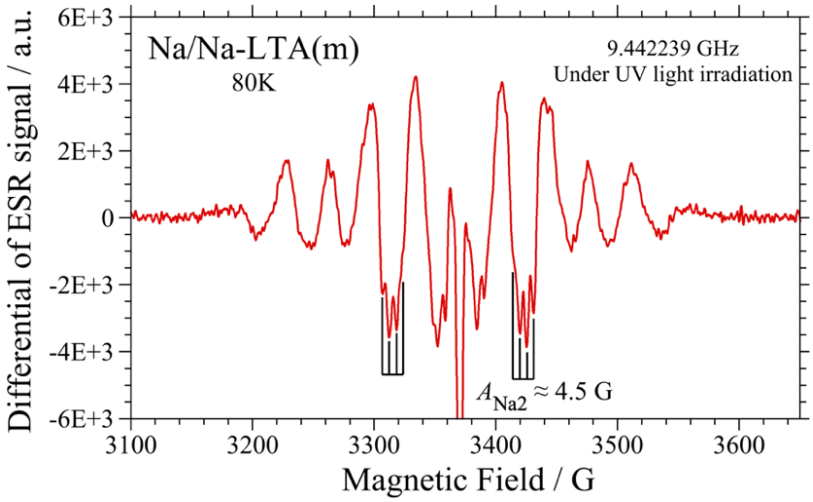

Fig. S13 Second derivative ESR spectrum of Na/Na-LTA(m) at 80 K under UV light irradiation derived from **Fig. 12**.

S6. Potential and electronic levels inside α- and β-cages of Na-LTA.

The energy potential inside α- and β-cages for doped electrons by the adsorption of Na atoms or phototransferred electrons is formed by several important factors. Attractive forces work between the electron and Na^+ ion and between the Na^+ ion and the negatively charged framework. A repulsive force works between the electron and the negatively charged framework. The attractive force between the electron and the Na^+ ion is the origin of the electron–phonon interaction. Furthermore, the Coulomb repulsive force works between the electrons in one Na cluster. It has been reported that a simplified model of a spherical quantum well with infinite depth, whose diameter is defined by the inner size of the cages, is a good approximation at the starting point to explain the electronic states of alkali metal clusters stabilized in zeolites.[S15] Electronic levels of 1s, 1p, 1d … appear in this quantum well in this order from the lower energy side. Considering the electron spins, 2, 6, 10 electrons can occupy these levels, respectively. The 1s and 1p levels appearing in the spherical (or cubic) quantum well can be expressed as A_{1g} and T_{1u}, which are the Mulliken symbols in group theory, respectively. The electronic transition between these levels is optically allowed and is the lowest in energy. Considering these points, the dependence of the optical transition between these levels on the spherical well diameter, d, was calculated as plotted in **Fig. 11**a by referring to Ref. S15.

The potential wells and the appearing electronic levels for the diamagnetic Na cluster in the β-cage and those for the photogenerated Na_4^{3+} cluster in the α-cage are illustrated in **Fig. 11**b and c. A detailed explanation of this figure is given in the main article.

References

S1 G. T. Kerr, Chemistry of Crystalline Aluminosilicates. II. The Synthesis and Properties of Zeolite ZK-4. *Inorg. Chem.*, 1966, **5**, 1537-1539.

S2 T. Kodaira and T. Ikeda, Characters of the Tetramethylammonium Ion in ZK-4 Zeolites Depending on Their Si/Al Ratios. *J. Phys. Chem. C* 2010, **114**, 12885-12895.

S3 R. L. Wadlinger, E. J. Rosinski and C. J. Plank, US Patent 3,375,205, 1968.

S4 A. Corma, F. Rey, J. Rius, M. J. Sabater and S. Valencia, Supramolecular self-assembled molecules as organic directing agent for synthesis of zeolites, *Nature* 2004, **431**, 287-290.

S5 M. M. Eddy, A. K. Cheetham and W. I. F. David, Powder Neutron-Diffraction Study of Zeolite Na-ZK-4; an application of new functions for Peak Shape and asymmetry. *Zeolites* 1986, **6**, 449-454.

S6 T. Ikeda, T. Kodaira, T. Oh and A. Nisawa, K^+ ion distribution in zeolite ZK-4's with various Si/Al ratios and the contribution of K^+ ions to K cluster formation. *Microporous Mesoporous Mater.*, 2003, **57**, 249-261.

S7 T. Ikeda, F. Izumi, T. Kodaira and T. Kamiyama, Structural study of sodium-type zeolite LTA by combination of Rietveld and maximum-entropy methods. *Chem. Mater.* 1998, **10**, 3996-4004.

S8 J. Ward, The nature of active sites on zeolites: I. The decationated Y zeolite. *J. Catal*., 1967, **9**, 225-236.

S9 D. Eisenberg and W. Kauzmann, *The Structure and Properties of Water*, Oxford University Press, London, 1969.

S10 T. Kodaira, Y. Nozue and T. Goto, Optical Absorption Spectra of Sodium Clusters Incorporated into Zeolite LTA. *Molec. Cryst. Liq. Cryst.*, 1992, **218**, 55-60.

S11 H. Pick, Structure of trapped electron and trapped hole centers in alkali halides "color centers" (Chapter 9) in *Optical properties of solids*, ed. F. Abelès, North-Holland Publishing, Amsterdam, 1972, pp. 653-754.

S12 T. Kodaira and Y. Murakami, Dependence of electron transfer among α cages on the chemical compositions of zeolite LTAs including K clusters. *J. Chem. Phys.* 2007, **127**, 094704.

S13 D. L. Dexter, Absorption of Light by Atoms in Solids. *Phys. Rev.* 1956, **101**, 48-55.

S14 C. Karunakaran and M. Balamurugan, Electron Paramagnetic Resonance Spectroscopy (Chap. 4) in *Spin Resonance Spectroscopy: Principles and Applications,* Karunakaran, C. Ed.; Elsevier, Amsterdam, 2018; pp. 169-228.

S15 T. Nakano and Y. Nozue, Electrons of alkali metals in regular nanospaces of zeolites. *Adv. Phys.: X*, 2017, **2**, 254-280.